Recent Measurements and Plans for the SLAC Compton X- Ray Source

A.E. Vlieks*, R. Akre*, G. Caryotakis*, C. DeStefano#, W.J. Frederick#, J.P. Heritage#, N.C. Luhmann Jr. #, D. Martin*, and C. Pellegrini§

SLAC- MS 33, 2575 Sand Hill Rd, Menlo Park, CA 94025, USA
#University of California, Davis, CA 95616, USA
§Department of Physics and Astronomy, UCLA, Los Angeles

Abstract. A compact source of monoenergetic X-rays, generated via Compton backscattering, has been developed in a collaboration between U.C Davis and SLAC. The source consists of a 5.5 cell X-band photoinjector, a 1.05 m long high gradient accelerator structure and an interaction chamber where a high power (TW), short pulse (sub-ps) infrared laser beam is brought into a nearly head-on collision with a high quality focused electron beam. Successful completion of this project will result in the capability of generating a monoenergetic X-ray beam, continuously tunable from 20 - 85 keV.

We have completed a series of measurements leading up to the generation of monoenergetic X-rays. Measurements of essential electron beam parameters and the techniques used in establishing electron/photon collisions will be presented.

We discuss the design of an improved interaction chamber, future electro-optic experiments using this chamber and plans for expanding the overall program to the generation of Terahertz radiation.

Keywords: Compton X-rays, RF gun, Optoelectric, Terahertz
PACS: 41.60.-m, 41.75.Ht, 41.75Lx.

INTRODUCTION

The Compton X-Ray source consists of a 5.5 cell X-band photoinjector, 1.05m long linear accelerator section developed in the NLC program [1] precision spectrometer, and Ti:Sapphire laser system. Its purpose is to generate nearly monoenergetic X-rays by colliding a beam of electrons, head-on, with a beam of photons as a proof-of –principle experiment for cancer diagnosis and treatment by Photon Activation therapy (PAT) using a room-sized facility. The X-rays generated will have energies, continuously tunable from 20-85 keV. During the past year of operation, the properties of the electron beam and laser system have been measured and are reported herein. These properties include beam energy, energy dispersion, and beam size. In addition, techniques to measure temporal and spatial alignment of the two beams have been developed.

A new improved interaction chamber has been designed and built during the last six months. Its purpose is to simplify temporal alignment for the collision of the electron and laser beams. In addition, the new chamber will permit the measurement of the

Contributed to 7th Workshop on High Energy Density and High Power RF, 13-17 June 2005, Kalamata, Greece

Work supported in part by Department of Energy contract DE-AC02-76SF00515

electron beam length using a nonlinear crystal to observe the change in polarization of a laser beam via the optoelectric effect due to an electron bunch.[2]

We have also been investigating the possibility of using the photoinjector for generating high peak power, coherent terahertz radiation.

EXPERIMENTAL SETUP/OPERATION

The experimental arrangement is shown in Fig. 1. Except for the high power klystrons and driver TWT's, all components are located in a radiation shielded room. The timing/frequency reference for the system originates from a short-pulse, Ti:Sapphire laser oscillator which operates at a repetition frequency of 79.33 MHz. A photodiode samples this frequency and supplies a signal to a 144X frequency multiplier. The resultant 11.424 GHz signal then serves as the reference frequency for the klystrons. The oscillator also supplies a seed pulse for the regenerative (Regen) amplifier. The output of the Regen is split into two paths. Half the energy supplies a seed signal for a 5-pass Ti:Sapphire amplifier and the other half enters a UPAZ Time-Plate (BBO)

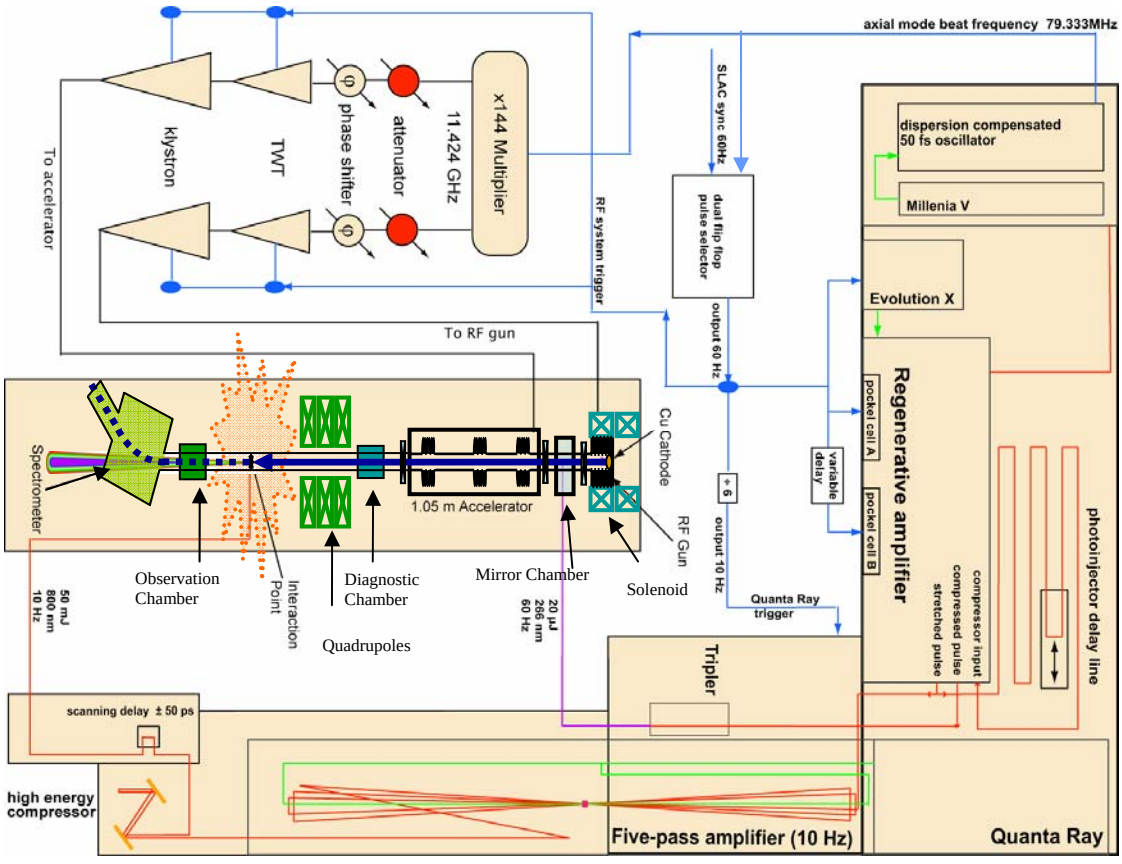

Figure 1. Compton X-Ray Source Setup

frequency tripler which reduces the 800 nm input signal to 266 nm. This UV signal generates the photoelectrons for the RF gun.

The RF Gun is a 5.5 cell standing wave structure[3,4]. The RF power enters symmetrically through the final cell. It is normally run at or near its design field gradient of 200 MV/m at the copper cathode. Figure 2 shows images of the electron beam on a Ce:YAG crystal for two different rf field strengths. The observation point is from the *Mirror Chamber* located at the exit of the gun. Note that the crystal becomes highly saturated at the higher rf field strength. The rectangular shadow at the right of each image is the UV mirror which directs the laser light onto the cathode. The pale streamers emanating from the beam spot are caused by dark current.

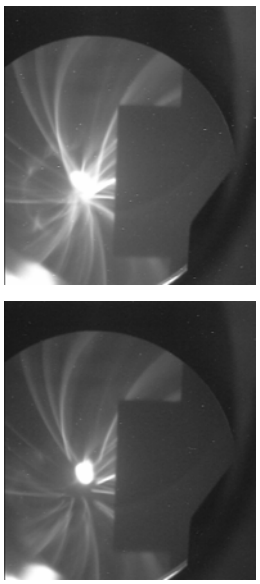

Surface Gradient (MV/m)	Electron Energy (MeV)
200	**7.3**
186	**6.8**

Figure 2. Electron beam images at exit of RF Gun.

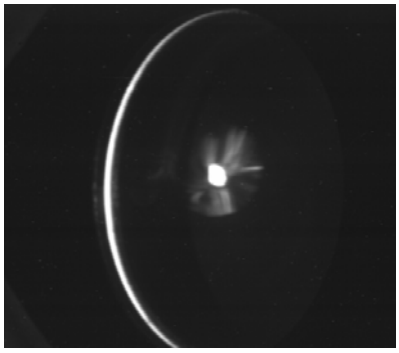

Following this diagnostic, the electron beam enters the 1.05 m long accelerating structure where it is accelerated up to 60 MeV. The beam may be viewed with a Ce:YAG crystal at the exit of the accelerator before it is focused by a triplet of quadrupoles. Figure 3 shows a typical image. The bright spot in the center is the electron beam, and the dim circle surrounding it is an image of the accelerator exit beam pipe. The large arc is the result of internal reflection on the Ce:YAG crystal

Figure 3. Electron beam image at the exit of the accelerator.

The electron beam is then focused to a small spot at the *Interaction Chamber* for collision with the laser beam. In order to align the two beams temporally, an Aluminum prism is inserted into the beam paths and measurements of light from the laser and optical transition radiation (OTR) from the electron beam are brought into coincidence (to within a few ps.) using a fast (160 ps) photomultiplier (PMT) and a 6 GHz Infinium Oscilloscope from Agilent Technologies. The electron beam OTR image on this prism viewed with a CCD camera is shown in Fig. 4. The speckles also seen on the CCD image are due to Bremstrahlung X-rays generated at the Prism. The laser beam is not present in this image

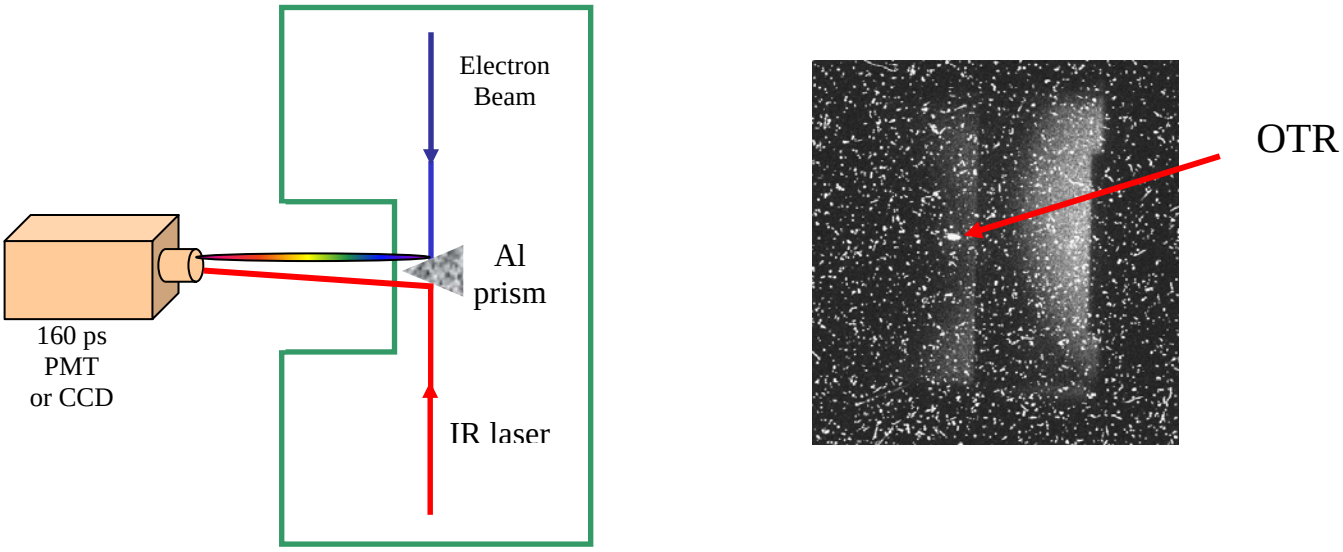

Figure 4. Schematic of temporal alignment procedure and actual CCD image.

After passing through the interaction chamber, the electron beam enters the *Observation Chamber*. This chamber contains two insertable diagnostics. These are an Aluminum Pellicle mounted at 45º to the beam path and a Ce:YAG crystal. The Aluminum Pellicle is used to focus the electron beam and provide accurate beam size determination via OTR. Results from these measurements are shown in a later section.

The electron beam then enters a spectrometer (see Fig. 5) where it is diverted to a 45º off-axis Faraday Cup while permitting measurement of the Compton X-radiation along the straight-through path.

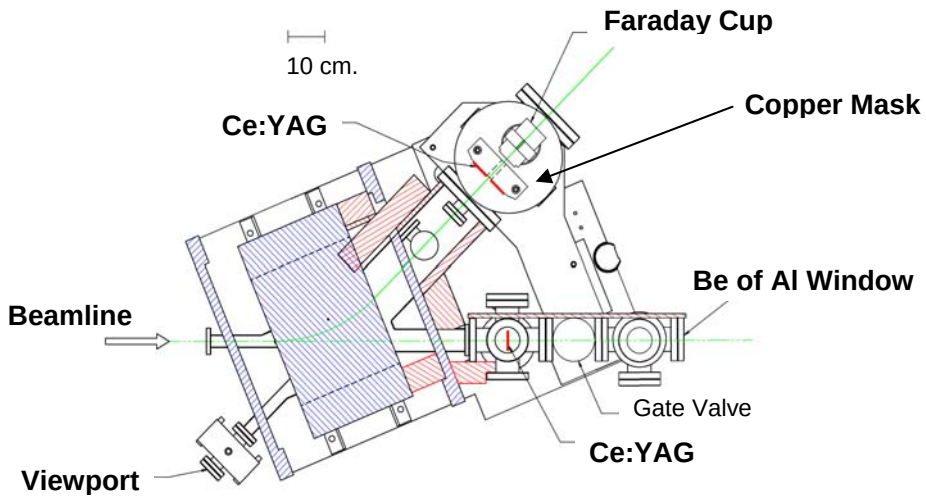

Figure 5. Electron spectrometer.

The Off-axis Faraday cup is equipped with a 5 cm thick Copper mask with a 1% energy slit. This allows measurement of electron beam current in 1% energy increments and permits measurement of beam energy resolution. On each side of the slit are mounted Ce:YAG crystals, viewable by a CCD camera through a viewport. This diagnostic permits location and shape of the analyzed beam in the electron spectrometer.

ELECTRON BEAM PARAMETER MEASUREMENTS

Using the diagnostics described above, we have measured important beam and RF Gun parameters and are able to compare these results with expectations. Initial beam emittance measurements have been described elsewhere. [4]

Electron Beam Energy and Energy Resolution

The electron beam energy and energy resolution were measured using several of the features of the spectrometer. The electron spectrometer was calibrated several years ago. Before beginning the current series of measurements, the magnetic field current and resulting magnetic field, measured via an embedded Hall probe, were compared with the earlier calibrations and found to be unchanged.

The electron beam energy was easily measured by passing it through the 1% energy slit. This was done at several energies. The resultant energy values were compared with predictions using known properties of the accelerator and RF Gun. In all cases, the measured results were approximately 95% of predicted values. The energy resolution was determined using two methods. In one case, the beam was moved to one side of the analyzing slit and its profile was measured using a CCD camera and frame-grabber. This is shown in Figs. 6a and 6b. In Fig. 6a, snapshots are shown of the beam on the Ce:YAG crystals, (left to right) when the magnetic field is too strong,

correct and too weak for the beam energy. The fuzzy spots above and below the main beam spot are due to light reflections from the chamber walls. Taking an intensity profile on the low energy image using a CCD camera and frame-grabber, the rms energy width was determined assuming a Gaussian profile. This is shown in Fig. 6b.

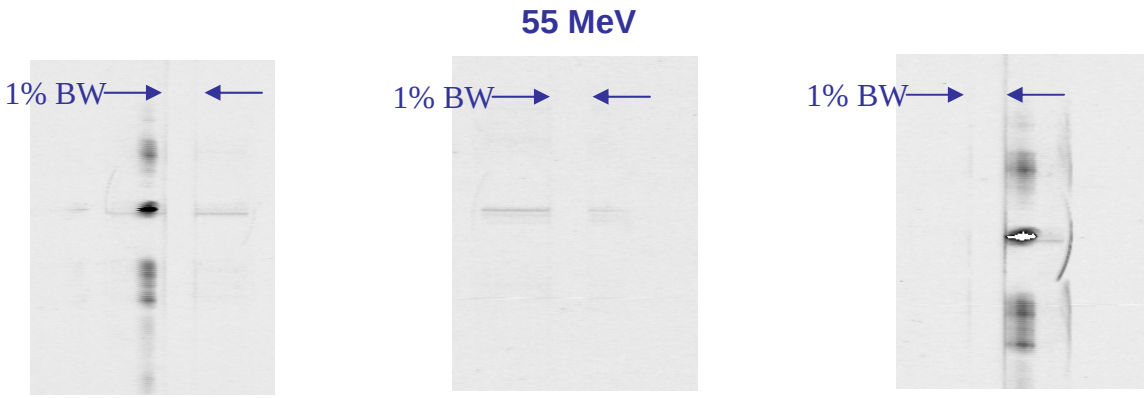

Figure 6a. Snapshots of electron beam in spectrometer. Arrows show 1% energy slit.

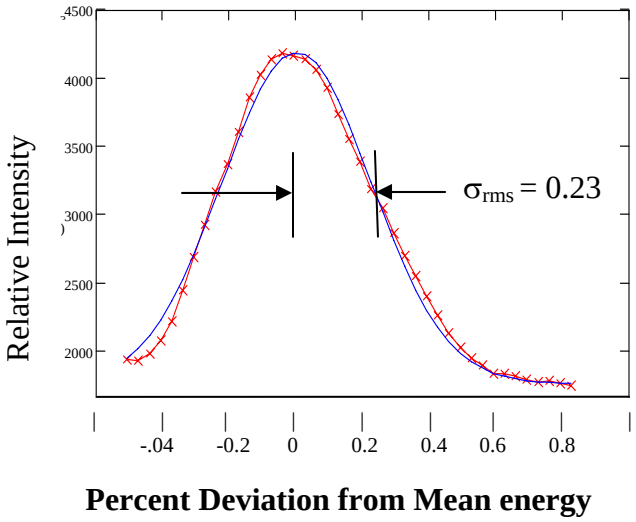

Figure 6b. Experimental and Fit to beam profile

The other method was to use one side of the slit as a knife-edge and move the electron beam into the slit in steps, measuring the analyzed beam current in each step. The resultant profiles were fit assuming a Gaussian energy distribution. The results are shown in Fig. 7.

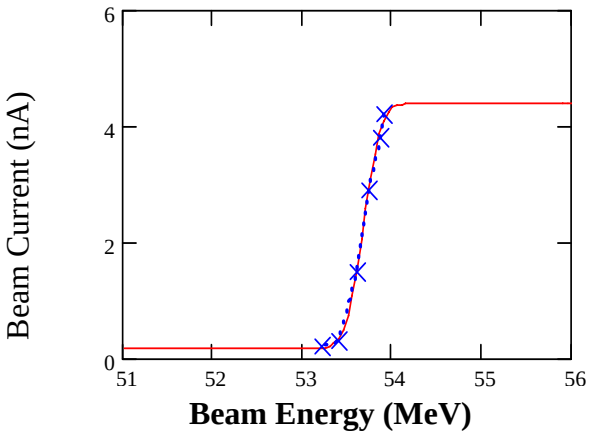

Fitting Function:

$$F(x) = A \cdot \left[1 + Erf\left(\frac{x-\mu}{\sqrt{2}\sigma}\right)\right] + B$$

Figure 7. Measured points and resultant fit. Resultant σ is 0.28%

Electron Beam Size Determination

The electron beam size was measured by observing the OTR from the electron beam on an Aluminum Pellicle in the *Observation Chamber* with a CCD camera. The image was captured by a frame-grabber and fit with a Gaussian profile. The measured points and fit are shown in Fig. 8.

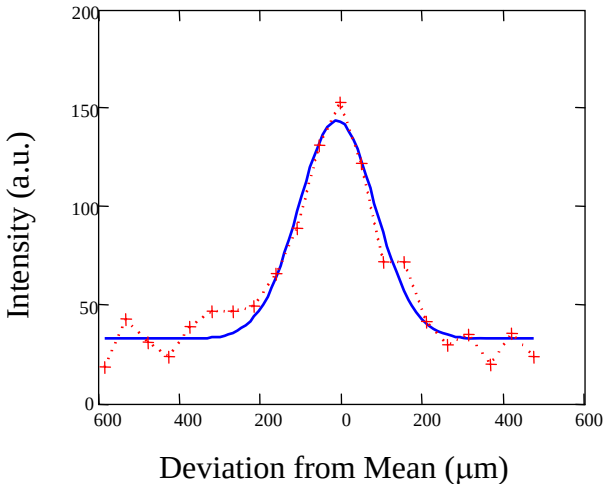

Figure 8. Electron beam size as determined from OTR measurement.

Electron Beam Current and Photocathode Quantum Efficiency

The spectrometer Faraday cup was used to measure analyzed electron beam current for different UV energies. This current was compared with measurements from an in-line Faraday cup located at the end of the beamline. Since this latter current measurement also contains dark–current contributions, an additional measurement was made with the laser off to find the dark current contribution. (In the spectrometer

current measurements there was essentially no current contribution, above noise, with the laser off.). The results are shown in Table 1.

Total In-line Current (nA)	Dark Current Contribution to In-line current (nA)	Net In-line Current (nA)	Spectrometer Analyzed Current (nA)
5.6	.99	4.6	4.5
10.5	1.4	9.1	9.0

Table 1. Comparison of beam current measured in Spectrometer with in-line current.

As can be seen, the agreement is excellent. The UV laser energy was also measured using an *EPM 2000 Laser Energy/Power Meter*. The resultant Quantum Efficiency is $5.3 \cdot 10^{-5}$. (Possible UV losses in the vacuum window and mirror were neglected)

DESIGN OF A NEW INTERACTION CHAMBER

In the current setup, the electron and laser beams collide at an angle of ≈162º. This requires the timing to be extremely precise (< 1ps) for *any* collision to take place. To alleviate this tight temporal tolerance, it was decided to design a new chamber in which the beams would collide head-on rather than obliquely. In order to accomplish this, the electron beam must either be diverted (by a magnet) so as not to hit the laser mirror or it must pass through a hole in the mirror. We have chosen the latter option because of its simplicity. The new chamber will replace the current interaction chamber and observation chamber. In addition, the floor of the chamber will consist of a vacuum-compatible breadboard to permit the inclusion of additional optical components. This chamber will be available for use this Fall.

One of the first experiments with this chamber will be to measure the pulse length of the electron beam by means of the Opto-electric effect on a birefringent crystal. A ZnTe crystal will be positioned under the electron beam path. The change in polarization (due to the electron beam) of a laser beam passing through the crystal will be used to measure the electron pulse length.

TERAHERTZ RADIATION

It is interesting to consider the capability of the current RF gun if it were used as a source of electrons for a Magnetic Undulator and what it would take to modify the experimental area into a user facility for high power, narrow band Terahertz radiation. The setup would consist of replacing the accelerator or adding a separate beam path equipped with a magnetic Undulator to the current beamline. The expected Terahertz power levels are illustrated in Table 2 for an undulator with a 12 period, 4.1cm/period Undulator operating at either 0.5 or 1.0 T. The current capability, for a 100μm pulse length would be 1-5 mW of average power. In order to reach a higher average power, multibunch operation would be incorporated and a newer laser amplifier is necessary.

Currently, 10 mJ@ 800 nm Ti:Sapphire Laser Amplifiers are available with repetition rates > 1 kHz.

Mode	rep rate (pps)	Laser energy/pulse (UV)	Bunches/ macropulse	Peak Power (@ B_0=0.5, 1.0 T)	Average Power
Current capability	**120**	**50 µJ**	**1**	**6.5 kW@ 1.1THz 28 kW@ 0.38 THz**	**1.3 mW 5.4 mW**
Multi-bunch operation	**120**	**1 mJ**	**16**	**10 kW@ 1.1THz 43 kW@ 0.38 THz**	**32 mW 135 mW**
High Rep rate Sheet beam Klystron	**1000**	**1mJ**	**16**	**10 kW@ 1.1THz 43 kW@ 0.38 THz**	**265 mW 1.1 W**
Advanced Cathode (Ce_2Te QE=1%)	**1000**	**50 µJ**	**16**	**1 MW@ 1.1THz 4.3 MW@ 0.38 THz**	**26 W 112 W**

Table 2. Availability of Terahertz Power

A simple, highly efficient means of obtaining multiple laser pulses for each RF macropulse is shown in Fig. 9. This method, consisting of a series of beam splitters and coated mirrors, permits the generation of 16 micro bunches per RF macro pulse. To increase the Terahertz power further, the RF power source must operate at a higher repetition rate. Investigation into the feasibility of a gridded Sheet-beam Klystron is being investigated at SLAC[5].

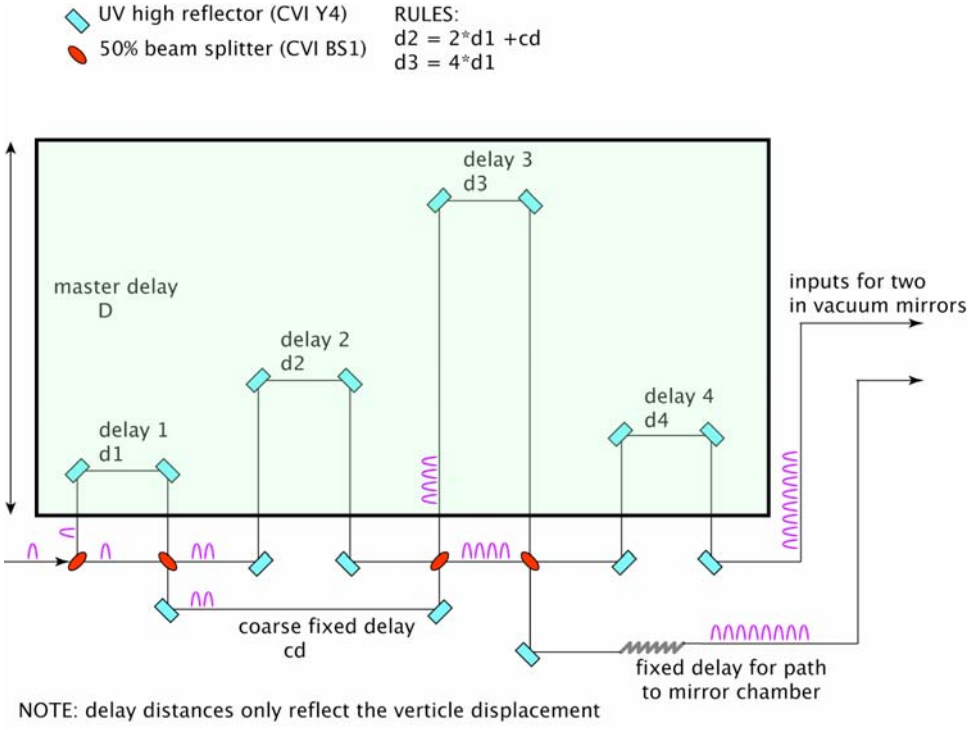

Figure 9. Generation of 16 UV micro pulses using a series of beam splitters and mirrors.

SUMMARY

The essential parameters of the X-Band Photoinjector have been measured and compare well with design specifications. This summer, we expect to generate X-rays and perform initial Opto-electric measurements. A new Interaction Chamber has been designed and built. Installation will commence this Fall. Plans are underway for modifying/expanding the current setup to permit generation of terahertz radiation.

REFERENCES

[1] C. Adolphsen,*"Advances in Normal conducting Accelerator Technology from X-Band Linear Collider Program"*, SLAC-PUB-11224, (June 2005), and Particle Accelerator Conference, Knoxville TN, May 16-20, 2005

[2] P.Bolton, D. Dowell, P.Krejcik, J. Rifkin, *"Techniques for electro-Optic Bunch Length Measurement at the Femtosecond Level*", SLAC-PUB- 9529 (October 2002)

[3] A.E.Vlieks et *Al*, "Development of an X-band RF Gun at SLAC", *High Energy Density and High Power RF*, 5th Workshop on High Energy Density and High Power RF, Snowbird, Utah. 2001, p107

[4]A.E.Vlieks et *Al*, "Initial Tests with an X-band Photoinjector at SLAC", *High Energy Density and High Power RF*, 6th Workshop on High Energy Density and High Power RF, Berkeley Springs, WV. 2003, p358

[5]V. Ivanov *et Al. "3D Modeling Activity For Novel High Power Electron Guns at SLAC"*, SLAC-PUB-10080 (July 2003)